Applied Physics Letters

RESEARCH ARTICLE | JULY 15 2024

THz generation by AlGaAs/GaAs heterostructured *p-i-n* diode

V. Trukhin ; I. Mustafin ; V. Malevich; X. Fan ; V. Kalinovskii; E. Kontrosh ; K. Prudchenko

Appl. Phys. Lett. 125, 031101 (2024)
https://doi.org/10.1063/5.0218713

AIP Publishing

Applied Physics Letters ARTICLE pubs.aip.org/aip/apl

THz generation by AlGaAs/GaAs heterostructured *p-i-n* diode

Cite as: Appl. Phys. Lett. **125**, 031101 (2024); doi: 10.1063/5.0218713
Submitted: 13 May 2024 · Accepted: 5 July 2024 ·
Published Online: 15 July 2024

V. Trukhin,[1,2,a)] I. Mustafin,[1] V. Malevich,[3,4] X. Fan,[1,2] V. Kalinovskii,[1] E. Kontrosh,[1] and K. Prudchenko[1]

AFFILIATIONS

[1]Ioffe Institute, St Petersburg, Russia
[2]ITMO University, St Petersburg, Russia
[3]Belarusian State University of Informatics and Radioelectronics, Minsk, Belarus
[4]Stepanov Institute of Physics, Belarusian Academy of Sciences, Minsk, Belarus

[a)]**Author to whom correspondence should be addressed:** valera.truchin@mail.ioffe.ru

ABSTRACT

The generation of terahertz radiation by heterostructure *p-i-n* $Al_xGa_{1-x}As$/GaAs diodes excited by femtosecond optical pulses was studied experimentally and using the Monte Carlo method. It is shown that when the reverse bias varies, the terahertz generation mechanism changes. With a positive bias on the *p-i-n* diode, the THz generation mechanism is due to the reflection of the photoexcited electrons from the interface. With a large internal electric field, THz generation in the *p-i-n* diode occurs due to the acceleration of electrons at the ballistic stage of their movement in the electric field to velocities significantly exceeding the steady state velocity ("velocity overshoot"). The subsequent sharp decrease in velocity of electrons is associated with their inter-valley transitions from the Γ-valley to the L-valley of the conduction band. At electric fields less than 22 kV/cm, the effect of electric field screening by photoexcited carriers has a significant impact on the formation of photocurrent and, accordingly, on the THz generation mechanism. As the reverse bias decreases, this effect leads to a shift in the maximum of the THz pulse toward shorter times and it begins to dominate at electric fields less than 10 kV/cm.

One of the new directions in the development of diagnostic technologies is terahertz coherent spectroscopy based on coherent methods of generation and detection of THz radiation in semiconductor structures using ultrashort femtosecond laser pulses. In this connection, many scientific groups conduct research on the processes of generation and detection of THz radiation in various media in order to create efficient coherent terahertz emitters and detectors for application in THz time-resolved spectroscopy systems. Semiconductor photoconductive antennas (PCAs) and InAs bulk semiconductors are mainly used as terahertz emitters. The photoconduction material in PCAs is typically composed of specially semiconductors (GaAs, InGaAs), which are grown by molecular beam epitaxy at reduced temperature or are specially doped to reduce the carrier lifetime.[1,2] Further improvement of THz emitters is associated with the use of structures based on metasurfaces (plasma excitation) and *p-i-n* diodes.[3] The first work to investigate THz generation in a silicon *p-i-n* diode was done by Auston's group.[4] The effect itself was explained by the electric field dependence of the drift velocity of photogenerated carriers in the *i*-region of the *p-i-n* diode. In subsequent works, for example, Nevinskas *et al.* studied THz emission from *p-i-n* GaInAs structures grown by the MBE method on InP substrates under excitation by femtosecond laser pulses.[5] It was demonstrated that the primary physical mechanism of this effect is the burst of photocurrent in the electric field of the *p-i-n* junction. Furthermore, it was demonstrated that GaInAs *p-i-n* diodes can achieve THz generation efficiency that is 2–3 times higher than that of *p*-InAs semiconductors excited by 800 nm radiation, which is known to be the most efficient THz emitter among bulk unstructured semiconductors at surface excitation in mirror geometry.[6]

The most recent review of promising THz range emitters considered various semiconductor structures: *p-i-n* diode junctions and plasmonic nanostructures.[3] These structures do not use semiconductor materials with short carrier lifetimes, as the authors of the review noted that despite the possibility of such emitters in a wide spectral range, subpicosecond photocarrier lifetimes lead to a significant loss of optoelectric gain and optical sensitivity. Furthermore, the synthesis of semiconductors with small carrier lifetimes necessitates the use of rare elements and nonstandard, technologically complex synthesis processes with limited availability.

Thus, semiconductor structures based on heterostructured *p-i-n* diodes of III-V semiconductors stand out as coherent THz sources.[4,5]

They possess a remarkable property—the ability to accelerate electrons in the region of the undoped semiconductor in large electric fields to velocities much higher than the saturation velocity, with subsequent rapid decline in the electron velocity due to inter-valley transitions of electrons from the Γ-valley to the L-valley leading to effective THz generation. The subpicosecond photocurrent pulse resulting from these processes creates an electric dipole that emits THz signal.[7–11] Creation of an effective THz emitter based on heterostructured *p-i-n* diodes of III-V semiconductors imposes certain requirements both on the design of the structure itself and on the establishment of the influence of such nonlinear-optical effects as self-induced light transparency, dynamic Burstein–Moss effect, processes related to shielding of the applied electric field by both THz radiation and spatial separation of charge carriers, as well as domain instability, on the process of THz generation. The above processes can lead to a decrease in the efficiency of THz generation.

This paper presents the results of experimental study and Monte Carlo simulation of terahertz radiation generation by $Al_xGa_{1-x}As$/GaAs heterostructured *p-i-n* diodes under excitation by femtosecond optical pulses.

Experimental samples of $Al_xGa_{1-x}As$/GaAs heterostructured *p-i-n* diodes were grown by molecular beam epitaxy (STE3526, SemiTEq) on 2 in. *n*-GaAs (001) substrates. Si(*n*) and Be(*p*) were used as doping impurities. The investigated structure included an *n*-GaAs buffer layer ($1 \times 10^{18}\,cm^{-3}$), an AlAs/GaAs Bragg grating (BG), an undoped *i*-GaAs layer ($n \approx 10^{15}\,cm^{-3}$) 1.5 μm thick, a 1.5 μm thick *p*-$Al_{0.1}Ga_{0.9}As$ layer ($p = 8 \times 10^{18}\,cm^{-3}$), a 0.1 μm thick p-$Al_{0.8}Ga_{0.2}As$ wide-area window ($p = 5 \times 10^{19}\,cm^{-3}$), and a p^+-GaAs contact layer ($p = 1 \times 10^{20}\,cm^{-3}$). Schematic and the band structure of the *p-i-n* diode are shown in the Figs. 1(a) and 1(b). On the grown epitaxial wafer, *p-i-n* diode chips with a total area of 1 mm^2 were formed using photolithography. A ring-shaped Ohmic contact was formed on the frontal photosensitive surface of the 200-μm-diameter chips using photolithography, followed by removal of the p^+-GaAs contact layer inside the ring.

The process of terahertz generation was studied by time-resolved terahertz spectroscopy. Titanium–sapphire lasers generating optical pulses of ~15 fs duration (at a wavelength of ~800 nm) and 100 fs duration (reconstructed to match the wavelength) were used to excite the studied samples. THz radiation was recorded using the electro-optical gating method in specular reflection geometry (a 1 mm thick ZnTe crystal was used).

While investigating the terahertz generation process by the *p-i-n* AlGaAs/GaAs diode, it was found that the THz pulse waveform (amplitude, duration, peak position) depends significantly on both reverse bias and excitation level as well as excitation wavelength. Figure 2(a) shows the waveforms of THz pulses generated by the *p-i-n* diode at reverse bias from 0 to −7.5 V excited by optical pulses with wavelength of 793 nm and 100 fs duration and at the average power of 8 mW. We can see that the maximum amplitude of the pulse increases as the reverse bias value on the diode increases and the time position of the pulse also changes.

Figure 2(b) illustrates the dependence of THz pulse delay and THz pulse amplitude on the bias for two excitation wavelengths. It can be observed that the maximum amplitude of the pulse increases rapidly with increase in reverse bias on the diode, and the onset of this growth depends on the excitation wavelength. The temporal position of the pulse also undergoes a change in response to alterations in the reverse bias value on the diode. As the bias decreases from positive values to the values of the voltage on the diode, at which the sharp growth of the pulse amplitude begins, the delay of THz pulse increases. With further increase in reverse bias on the diode, a reverse shift of the THz pulse occurs on the time scale.

Thus, the delay time for the maximum amplitude of the THz pulse non-monotonically depends on the bias voltage on the diode. It can also be seen that the temporal shift of THz pulse depends on the wavelength of the exciting radiation: for higher energy light quanta, this shift occurs at higher reverse bias on the p-i-n diode.

The temporal dynamics of the subpicosecond photocurrent pulse of nonequilibrium carriers in the *p-i-n* diode was calculated using the ensemble Monte Carlo method, which takes into account the screening of electric field in the *i*-layer due to a spatial separation of electrons and holes. As shown earlier, the effect of field shielding by photoexcited carriers can affect the photocurrent dynamics, and at sufficiently large electron–hole plasma density, it—like inter-valley transitions of electrons—can lead to the effect of electron velocity burst.[12,13]

The Monte Carlo simulation results presented in Figs. 3(a) and 3(b) are consistent with experimental data. Indeed, it can be seen that the position of photocurrent maximum depends non-monotonically

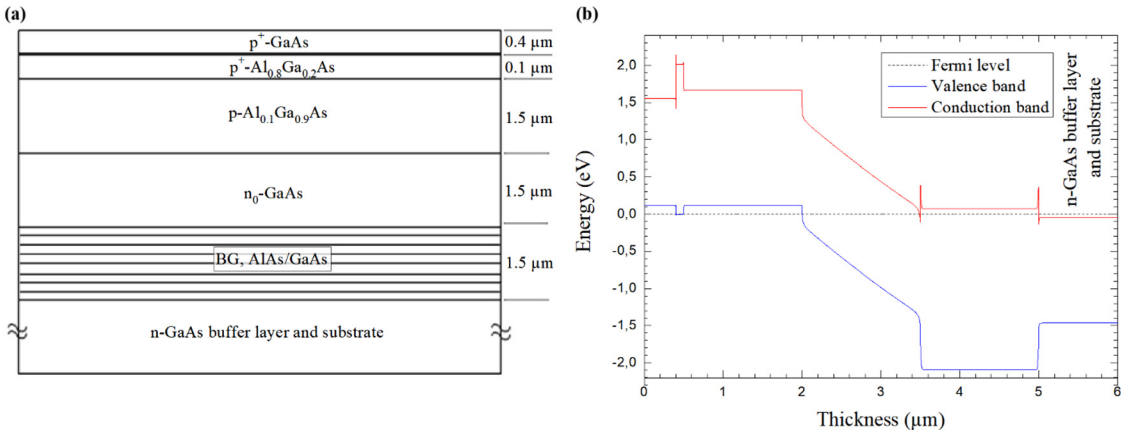

FIG. 1. (a) Schematic structure of the *p-i-n* diode; (b) band structure of the *p-i-n* diode.

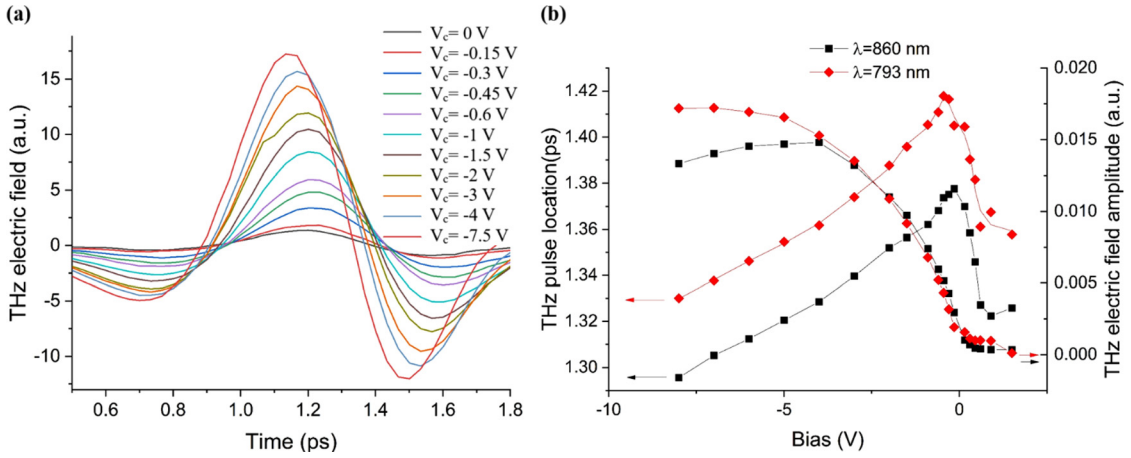

FIG. 2. (a) Waveforms of THz pulses generated in the p-i-n diode (V_c from 0 to −7.5 V, P = 8 mW, $\lambda = 793$ nm, $\tau = 100$ fs); (b) amplitude and position of THz pulses generated by the AlGaAs/GaAs p-i-n diode as a function of bias (P = 8 mW, $\tau = 100$ fs).

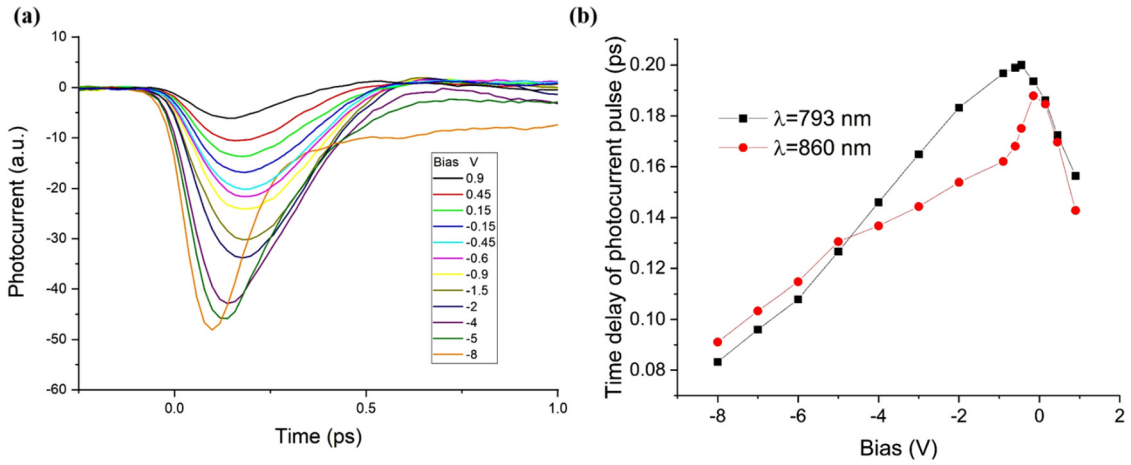

FIG. 3. (a) Calculated time dependencies of the photocurrent generated in the p-i-n diode (V_c from 0.9 V to −8 V, P = 8 mW, $\lambda = 793$ nm, $\tau = 100$ fs); (b) position of the maximum current amplitude in dependence on the bias (P = 8 mW, $\tau = 100$ fs).

on the bias, i.e., it demonstrates approximately the same dependence as the experimentally measured THz field in the far zone, which is defined as the time derivative of the photocurrent. The dependencies of the shift of the point in time, corresponding to the maximum value of the THz electric field, on the reverse bias, which are observed experimentally and follow from the results of Monte Carlo simulation, can be explained as follows.

When the diode is excited by femtosecond laser radiation, the formation of photocurrent pulse occurs within 100–300 fs, i.e., at the stage of the ballistic regime of electron motion. The rise time of the leading edge of the photocurrent is determined by the duration of the optical pulse and the magnitude of the accelerating electric field. The photocurrent decay and the formation of its trailing edge are determined by two mechanisms: (1) inter-valley transitions of electrons from Γ-valley to L-valleys and (2) screening of the electric field by photocarriers. The first photocurrent decay mechanism is responsible for the well-known velocity overshoot effect and occurs when the electric field is strong enough for the electron to reach the threshold energy for valley junctions before the electric field collapses due to the screening effect.

Let us consider a photoexcited electron accelerated under the action of a uniform electric field F. At the stage of ballistic motion, its velocity grows linearly with time t as $\upsilon(t) = eFt/m$, where m is the effective mass of the electron in the Γ-valley. Accordingly, the energy of a photoelectron is defined as $\varepsilon_0 + \frac{e^2F^2t_F^2}{2m}$, where $\varepsilon_0 \sim (\hbar\omega - \varepsilon_g)$ is the initial energy of the photoelectron (ω is the frequency of the optical radiation, ε_g is band energy gap). After a time $t_F = \sqrt{2m(\Delta - \varepsilon_0)}/(eF)$, the photoelectron in the Γ-valley reaches an energy Δ, corresponding to the threshold of transitions from Γ-valley to the subsidiary, highly effective mass L-valleys. The electron with such energy in a very short time of about 30 fs transfers into the side L-valleys of the conduction zone where its velocity drops sharply.[14] Therefore, the

electron accelerated by electric field will reach the maximum velocity at the moment when its energy reaches the threshold value Δ. Thus, with a decrease in reverse bias and, consequently, the electric field strength in the *i*-layer, the inter-valley mechanism of the photocurrent decay leads to a shift of its maximum toward longer times. For GaAs with the parameters $m = 0.067m_0$, $\Delta = 0.29$ eV under the excitation by pulses with a wavelength of 793 nm, the time required for the electron to gain the threshold energy decreases from 155 to 56 fs with increase in the reverse bias from 2 to 8 V. In this case, the time point corresponding to the maximum of photocurrent shifts by about 100 fs, which approximately corresponds to the shift value observed in the experiment. From Monte Carlo calculations [Fig. 3(b)], the delay times of 185 and 82 fs are obtained, which are slightly larger than the delay times given above. This distinction is due to the use of the simplest model for estimates, which does not take into account the nonparabolicity of the conduction band.

In the above reasoning, the effect of electric field screening by photoexcited carriers was not taken into account, i.e., it was assumed that the time t_F is less than the screening time $\tau_s = max(\tau_d, \omega_p^{-1})$, where $\tau_d = \left(\omega_p^2\tau\right)^{-1}$ is the dielectric relaxation time, τ is the electron pulse relaxation time, ω_p is the plasma frequency. For the *p*-*i*-*n* diode considered here, when the photocarrier density does not exceed 10^{15} cm^{-3}, the condition $t_F < \tau_s$ is satisfied for almost all reverse bias values. However, at the femtosecond pulse energy density used here, the electron–hole plasma density near the *p*-region reaches 5×10^{16} cm^{-3}, and the corresponding screening time is approximately 200–300 fs. Estimations show that in this case screening of the electric field will weakly affect the dynamics of the inter-valley transitions and the photocurrent pulse only at reverse bias values $(-V) > 2$ V, which corresponds to the electric field strength in the *i*-layer of about 22 kV/cm. It should be noted that in the stationary mode, when the screening effect is not taken into account, the threshold value of the electric field strength for inter-valley transitions in GaAs is about 3 kV/cm. At lower values of the reverse bias ($-V < 2$ V), inter-valley transitions of electrons practically do not occur, since the electric field collapses before the electrons gain threshold energy. In the ballistic mode, an electron in the time-varying electric field will accelerate and will reach maximum velocity at the instant when the field changes sign due to the screening effect. From this moment, the electric field begins to slow down the electrons. Thus, at low values of the electric field strength, when the electron does not have time to gain the threshold energy during the screening time, the decay time of the trailing edge of the photocurrent pulse is determined not by inter-valley transitions but by the shielding effect.

The above mechanism of the influence of screening process on the formation of photocurrent pulse assumes that the electric field in the i-layer remains almost homogeneous. In reality, the exponential character of photoelectron distribution in the i-layer, as well as the dependence of shielding time on their local concentration, will lead to inhomogeneity of the electric field distribution. The influence of inhomogeneity of the photoelectron concentration along the depth will be especially significant for excitation at a wavelength of 793 nm. In this case, the electron concentration at the i-layer length of 1.5 μm changes by almost an order of magnitude. From the Monte Carlo simulation results, it follows that near the p-layer the screening time is about 100–150 fs and increases to about 300–450 fs near the substrate. The different relaxation rate of the electric field causes the field strength near the substrate to be several times higher than the value of the field strength near the p-layer. Therefore, even at displacements of $-V < 2$ V, inter-valley transitions can occur in the region near the substrate where the field is still strong enough. Note that the mechanism associated with the velocity overshoot effect will manifest itself differently for optical radiation when the wavelength is changed. At excitation by optical pulses with a wavelength of 793 nm, the effective mass of the photoexcited electron will be much larger than the effective mass of the photoexcited electron at excitation with wavelengths of 860 and 827 nm. Accordingly, the onset of the "velocity overshoot" effect at 793 nm excitation will occur at a large value of reverse mixing, which can be seen in Figs. 2(b) and 3(b).

The Monte Carlo simulation shows that increasing the reverse bias results in increase in the screening time, i.e., screening a larger field takes longer. This dependence of the screening time on the external bias can be explained by the effect of heating electrons in the electric field, which leads to an increase in the average electron energy and, consequently, its effective mass. It follows that at low reverse bias values, when the inter-valley transitions do not occur and the screening effect is responsible for the decay of photocurrent pulse, the position of the photocurrent maximum will shift toward shorter times as the electric field decreases.

At positive bias, the electric field strength in the *i*-layer is small and the main contribution to the photocurrent is the reflection of photoexcited electrons from the interface. This mechanism of photocurrent generation known as "reactive" photoelectric effect is characterized by a large steepness of the leading edge of the photocurrent pulse, which consequently results in a small delay of the terahertz pulse.[15]

When considering the influence of the screening process on the dynamics of the photocurrent pulse, it was assumed that the electric field in the *i*-layer remains almost uniform. In fact, an exponential decrease in the photoelectron density in the *i*-layer leads to inhomogeneity of the electric field. From the results of Monte Carlo simulation, it follows that at 793 nm excitation, the field strength near the substrate is 2–3 times higher than the field strength near the *p*-layer, and even at the reverse bias $-V < 2$ V inter-valley transitions can occur in the region near the substrate, where the field is still quite strong.

Comparative studies of THz generation in the bulk semiconductor p-InAs were conducted, which demonstrated that the efficiency of THz generation in the *p*-*i*-*n* diode is approximately one order of magnitude higher than in *p*-InAs. Figure 4 illustrates the waveforms of THz pulses generated in the *p*-*i*-*n* diode and *p*-InAs. It is evident that the amplitude of the THz pulse generated in the *p*-*i*-*n* diode is four times greater than that of the THz pulse generated in p-InAs. Consequently, the energy superiority is more than an order of magnitude.

The obtained results allow us to propose a model for the generation of THz radiation in the *p*-*i*-*n* diode structure. Upon excitation of the pin-diode, nonequilibrium electrons and holes are generated in the i-region, which then move in the electric field. The holes move toward the p-AlGaAs region, while the electrons move toward the *n*-GaAs region. At a positive bias on the *p*-*i*-*n* diode, the THz generation mechanism is due to the reflection of photoexcited electrons from the interface. As the reverse bias increases (from +0.9 to −8 V), there is a change in the mechanism of formation of the rear edge of the photocurrent pulse, respectively, and the mechanism of THz generation. In the region of reverse bias from −8 to −2 V, inter-valley transitions occur almost along the entire length of the i-layer, resulting in the

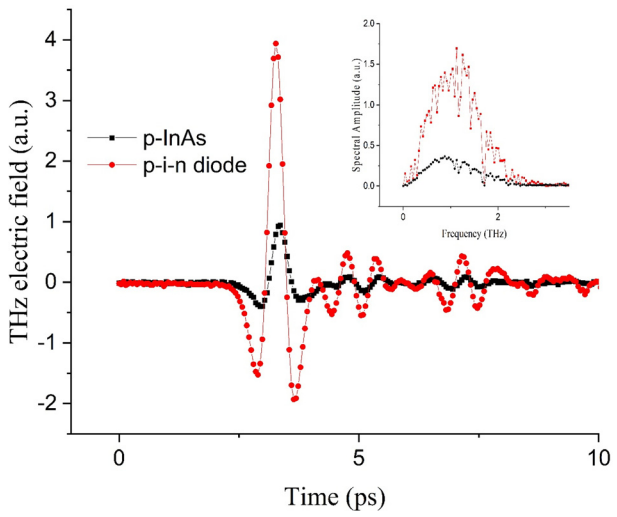

FIG. 4. Waveforms of THz pulses generated by p-i-n diode ($V_c = -8$ V) and p-InAs ($P = 3 \times 10^{16}$ cm^{-3}), ($P = 2$ mW, $\tau = 15$ fs) with corresponding spectra (in inset).

formation of photocurrent pulse via the velocity overshoot mechanism. As the reverse bias decreases, the photocurrent maximum shifts toward longer times. In the region from -2 to ~ -0.5 V ($\sim$10 kV/cm), the photocurrent maximum shifts in the same direction. This small shift ($\sim$20 fs) is also caused by inter-valley transitions, but in the region at the edge of the i-layer (near BG). At displacements from -2 to $+0.9$ V, the screening effect has a significant influence on the photocurrent formation. This phenomenon results in a shift of the photocurrent maximum in the opposite direction (to shorter times), which becomes pronounced at biases ranging from -0.5 to $+0.9$ V. The shift of the photocurrent maximum in the opposite direction is due to the fact that screening occurs faster as the electric field decreases.

Thus, the analysis of mechanisms of photocurrent formation and, accordingly, the generation of a THz pulse in the p-i-n diode performed by the ensemble Monte Carlo method made it possible to explain the non-monotonic behavior of the position of maximum amplitude of the THz pulse from the reverse bias as a result of changes in the mechanisms responsible for photocurrent relaxation. An ultrafast decrease in electric field in the i-layer due to the screening effect, which occurs in subpicosecond times scales, leads to an increase in the threshold value of reverse bias at which inter-valley transitions of photoelectrons from the Γ-valley to the L-valleys occur. In the absence of inter-valley transitions, the relaxation dynamics of the photocurrent pulse is determined by the screening of electric field due to a spatial separation of photoexcited electrons and holes.

AUTHOR DECLARATIONS

Conflict of Interest

The authors have no conflicts to disclose.

Author Contributions

V. Trukhin: Conceptualization (lead); Investigation (equal); Supervision (lead); Writing – original draft (lead); Writing – review & editing (lead). **I. Mustafin:** Data curation (equal); Investigation (equal); Writing – original draft (equal); Writing – review & editing (equal). **V. Malevich:** Data curation (equal); Investigation (equal); Writing – original draft (equal); Writing – review & editing (equal). **X. Fan:** Data curation (equal); Writing – original draft (equal). **V. Kalinovskii:** Conceptualization (equal); Investigation (equal); Writing – review & editing (equal). **E. Kontrosh:** Investigation (equal). **K. Prudchenko:** Investigation (equal).

DATA AVAILABILITY

The data that support the findings of this study are available from the corresponding author upon reasonable request.

REFERENCES

[1]R. B. Kohlhaas, S. Breuer, L. Liebermeister, S. Nellen, M. Deumer, M. Schell, M. P. Semtsiv, W. T. Masselink, and B. Globisch, "637 μW emitted terahertz power from photoconductive antennas based on rhodium doped InGaAs," Appl. Phys. Lett. **117**, 131105 (2020).
[2]M. Deumer, S. Breuer, R. Kohlhaas, S. Nellen, L. Liebermeister, S. Lauck, M. Schell, and B. Globisch, "Continuous wave terahertz receivers with 4.5 THz bandwidth and 112 dB dynamic range," Opt. Express **29**(25), 41819 (2021).
[3]P.-K. Lu, A. D. J. Fernandez Olvera, D. Turan, T. S. Seifert, N. T. Yardimci, T. Kampfrath, S. Preu, and M. Jarrahi, "Ultrafast carrier dynamics in terahertz photoconductors and photomixers: Beyond short-carrier-lifetime semiconductors," Nanophotonics **11**(11), 2661 (2022).
[4]L. Xu, X.-C. Zhang, D. Auston, and B. Jalali, "Terahertz radiation from large aperture Si p-i-n diodes," Appl. Phys. Lett. **59**(26), 3357 (1991).
[5]I. Nevinskas, A. Krotkus, S. Stanionytė, and V. Pačebutas, "Terahertz emission from GaInAs p-i-n diodes photoexcited by femtosecond laser pulses," Lith. J. Phys. **55**(4), 274 (2016).
[6]R. Adomavičius, A. Urbanowicz, G. Molis, A. Krotkus, and E. Šatkovskis, "Terahertz emission from due to the instantaneous polarization," Appl. Phys. Lett. **85**, 2463 (2004).
[7]A. Leitenstorfer, S. Hunsche, J. Shah, M. C. Nuss, and W. H. Knox, "Femtosecond charge transport in polar semiconductors," Phys. Rev. Lett. **82**, 5140 (1999).
[8]A. Leitenstorfer, S. Hunsche, J. Shah, M. C. Nuss, and W. H. Knox, "Femtosecond high-field transport in compound semiconductors," Phys. Rev. B **61**, 16642 (2000).
[9]P. Bowlan, W. Kuehn, K. Reimann, M. Woerner, T. Elsaesser, R. Hey, and C. Flytzanis, "High-field transport in an electron-hole plasma: Transition from ballistic to drift motion," Phys. Rev. Lett. **107**, 256602 (2011).
[10]G. H. Döhler, F. Renner, O. Klar, M. Eckardt, A. Schwanhäußer, S. Malzer, D. Driscoll, M. Hanson, A. C. Gossard, G. Loata, T. Löffler, and H. Roskos, "THz-photomixer based on quasi-ballistic transport," Semicond. Sci. Technol. **20**, S178 (2005).
[11]C. Müller-Landau, S. Malzer, H. B. Weber, G. H. Dohler, S. Winnerl, P. Burke, A. C. Gossard, and S. Preu, "Terahertz generation with ballistic photodiodes under pulsed operation," Semicond. Sci. Technol. **33**, 114015 (2018).
[12]A. E. Iverson, G. M. Wysin, D. L. Smith, and A. Redondo, "Overshoot in the response of a photoconductor excited by subpicosecond pulses," Appl. Phys. Lett. **52**, 2148–2150 (1988).
[13]K. Meyer, M. Pessot, G. Mourou, R. Grondin, and S. Chamoun, "Subpicosecond photoconductivity overshoot in gallium arsenide observed by electrooptic sampling," Appl. Phys. Lett. **53**, 2254 (1988).
[14]P. C. Becker, H. L. Fragnito, C. H. Brito Cruz, J. Shah, R. L. Fork, J. E. Cunningham, J. E. Henry, and C. V. Shank, "Femtosecond intervalley scattering in GaAs," Appl. Phys. Lett. **53**, 2089–2090 (1988).
[15]B. I. Belinicher and S. M. Ryvkin, "Jetlike photoelectromotive force in semiconductors," Sov. Phys. JETP **54**(1), 190 (1981).